# Sommerfeld and Zenneck Wave Propagation for a Finitely Conducting One-Dimensional Rough Surface

Akira Ishimaru, *Life Fellow, IEEE*, John Dexter Rockway, Yasuo Kuga, *Senior Member, IEEE*, and Seung-Woo Lee

***Abstract*—Starting with Zenneck and Sommerfeld wave propagation over a flat finitely conducting surface has been extensively studied by Wait and many other authors. In this paper, we examine propagation over a finitely conducting rough surface, also studied by many people including Feinberg, Bass, Fuks, and Barrick. This paper extends the multiple scattering theories based on Dyson and Bethe–Salpeter equations and their smoothing approximations. The theory developed here applies to rough surfaces with small root-mean-square (rms) heights ($\sigma < 0.1\lambda$). We limit ourselves to the one-dimensional (1-D) rough surface with finite conductivity excited by a magnetic line source, which is equivalent to the Sommerfeld dipole problem in two dimensions ($x$-$z$ plane). With the presence of finite roughness, the total field decomposes into the coherent field and the incoherent field. The coherent (average) field is obtained by using Dyson's equation, a fundamental integral equation based on the modified perturbation method. Once the coherent field has been obtained, we determine the Sommerfeld pole, the effective surface impedance, and the Zenneck wave for rough surfaces of small rms heights. The coherent field is written in terms of the Fourier transform, which is equivalent to the Sommerfeld integral. Numerical examples of the attenuation function are compared to Monte Carlo simulations and are shown to contrast the flat and rough surface cases. Next, we obtain the general expression for the incoherent mutual coherence functions and scattering cross section for rough conducting surfaces.**

***Index Terms*—Electromagnetic (EM) scattering from rough surfaces, Sommerfeld wave, Zenneck wave.**

## I. Introduction

WAVE propagation over a flat conducting earth excited by a dipole is a classic electromagnetic (EM) problem and has been studied by Wait and many others [1], [2]. Radio wave propagation over a rough surface was first studied by Feinberg [3], who obtained an effective impedance at the interface. Barrick conducted extensive studies on HF/VHF propagation over rough seas [4], [5] and showed that the spherical earth residue series model should be used for multiple frequency-very high frequency (MF-VHF) propagation over a rough sea. This was also shown rigorously by Wait [6]. The effective impedance of rough surfaces has been extensively studied by Bass *et al.* [7]–[9] using an extension of the small perturbation theory and the diagram method [10], [11]. Multiple scattering theories for rough surface scattering have also been proposed by Watson and Keller [12], [13], Ito [14] and Ishimaru *et al.* [15]. Further studies have been conducted recently for low grazing angle (LGA) scattering [16]–[19].

This paper follows and extends the multiple scattering theories developed by Bass *et al.* [8], [12]–[15]. Making use of the Feynman diagram method [10], [11], [21], the coherent field is shown to be expressed in the form of a Sommerfeld integral from which the Zenneck wave pole, effective surface impedance, and attenuation function for a rough conducting surface is obtained. The effective surface impedance is consistent with those obtained by Feinberg *et al.* in appropriate limits. The incoherent field and the scattering crosssections are shown to be similar to Watson–Keller [12], [13] and consistent with Fuks *et al.* [19] in the Neumann surface limit.

We consider a one-dimensional (1-D) finitely conducting rough surface excited by a magnetic line source located near the surface as shown in Fig. 1. The field at the observation point consists of the coherent and incoherent fields. The coherent field propagates over the flat surface with the equivalent reflection coefficient, which includes the effects of rough surface scattering. As the coherent field propagates over the rough surface, the field eventually diminishes and a part of the field is gradually converted into the incoherent (diffused) field. The incoherent field needs to be expressed in terms of the mutual coherence function which satisfies the fundamental Bethe–Salpeter equation. The coherent field is expressed in a Fourier transform which is equivalent to the Sommerfeld integral for a flat conducting surface. The pole of the reflection coefficient gives the propagation constant of the Zenneck wave over the rough conducting surface.

In order to include the rough surface effects, we start with the modified perturbation method and Dyson's equation [8], [12]–[15], which is a fundamental integral equation for the coherent field. We make use of the first-order smoothing approximation and solve Dyson's equation. The result is represented in the Fourier integral transform. The pole in the integral provides the propagation constant for the Zenneck wave. The coherent field can then be calculated using the rough surface Zenneck wave pole. The final expression for the field over the rough surface is given in terms of the "numerical distance." We present numerical examples of the Sommerfeld poles and the "attenuation function" for rough surfaces, and compare the results with Monte Carlo simulations showing good agreement. We also present a general formulation for the incoherent mutual coherence function and the scattering crosssections per unit length of the finitely conducting rough surface.

Manuscript received August 27, 1999; revised February 18, 2000. This work was supported by ONR Contracts N00014-97-1-0590 and N00014-00-1-0027 and NSF Contract ECS-9 908 849.

The authors are with the Department of Electrical Engineering, University of Washington, Seattle, WA, 98195-2500 USA (e-mail: ishimaru@ee.washington.edu).

Publisher Item Identifier S 0018-926X(00)09359-5.

0018–926X/00$10.00 © 2000 IEEE

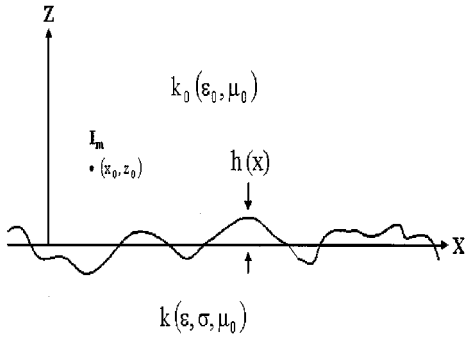


Fig. 1. Magnetic line current $I_m$ is located at $(x_o, z_o)$. Conducting medium is bounded by rough surface given by the height $h = h(x)$.

## II. Formulation of the Problem

Let us first consider the magnetic line source $I_m$ located at $x_o, z_o$ in free-space. The conducting half-space with permittivity $\epsilon$ and conductivity $\sigma$ is bounded by the rough surface whose height $h = h(x)$ is a random function of $x$, Fig. 1. The magnetic field has only the $y$-component and satisfies the wave equation. We let

$$H_y(x,z) = iw\epsilon_o I_m G(x,z). \tag{1}$$

Then the Green's function $G(x,z)$ satisfies

$$\left(\frac{\partial^2}{\partial x^2} + \frac{\partial^2}{\partial z^2} + k_o^2\right) G(x,z) = -\delta(x-x_o)\delta(z-z_o). \tag{2}$$

We next consider the boundary condition for $G(x,z)$. Here, we assume the first-order boundary condition that the ratio of the tangential electric field to the tangential magnetic field is the surface impedance $Z_s$ [1]. Thus, the Green's function satisfies the following condition on the surface $h(x)$.

$$\frac{\partial}{\partial n} G + \alpha_o G = 0 \tag{3}$$

where $\alpha_o = ik_o(Z_s/Z_o)$, $Z_o = \sqrt{\mu/\epsilon_o} =$ free-space characteristic impedance and $\partial/\partial n$ is the normal derivative. The surface impedance $Z_s$ is approximated by that of the flat conducting surface and is approximately given by [1]

$$\begin{aligned} Z_s &= \frac{Z_o}{n}\sqrt{1-\frac{1}{n^2}} = Z_o\Delta \\ n^2 &= \epsilon + i\frac{\sigma}{w\epsilon_o} \end{aligned} \tag{4}$$

where $n$ is the refractive index of the conducting medium. This is an approximation as the incident field approaches grazing. The problem is now reduced to the one medium problem (2) with the surface boundary condition of (3). In this paper, we use the time dependence $e^{-iwt}$. Now the surface $h(x)$ is a random function and, therefore, the field $G(x,z)$ is also a random function and consists of the coherent field $\langle G\rangle$ and the incoherent (or diffuse) field $G_d$ [10], [20]

$$G = \langle G\rangle + G_d. \tag{5}$$

## III. Equivalent Boundary Condition at $z = 0$

In order to include the effects of the rough surface, we use the modified perturbation technique [8], [15]. Compared with the conventional perturbation technique, this modified technique has a wider range of validity and also includes surface wave propagation due to the presence of pole. We now consider the boundary condition (3), which is valid at the surface $h(x)$. We write an equivalent boundary condition at $z = 0$ by expanding the Green's function about the surface height $h(x)$ and include only the first powers of $h$. First we note that

$$\frac{\partial}{\partial n} = \frac{-\frac{\partial h}{\partial x}\frac{\partial}{\partial x} + \frac{\partial}{\partial z}}{\left(1+\left(\frac{\partial h}{\partial x}\right)^2\right)^{1/2}} \approx -\frac{\partial h}{\partial x}\frac{\partial}{\partial x} + \frac{\partial}{\partial z} + \cdots \tag{6}$$

$$G(x,z) = G(x,o) + h(x)\frac{\partial}{\partial z}G + \cdots. \tag{7}$$

Therefore, the equivalent boundary condition (3) for the rough surface is now expressed at $z = 0$ up to first-order $h$

$$\frac{\partial}{\partial z}G + \alpha_o G + VG = 0 \tag{8}$$

where the random surface potential $V$ is given by

$$V = h\frac{\partial^2}{\partial z^2} - \frac{\partial h}{\partial x}\frac{\partial}{\partial x} + h\alpha_o\frac{\partial}{\partial z}.$$

## IV. Random Integral Equation for $G(r, r_o)$

We now develop the integral equation for the rough surface Green's function at the equivalent surface $z = 0$. Starting with Green's Theorem

$$\int_s \left(u\nabla^2 v - v\nabla^2\right) ds = \oint_c \left(u\frac{\partial v}{\partial n} - v\frac{\partial u}{\partial n}\right) dl \tag{9}$$

we let $u = G$ and $v = G_o$. $G_o$ is the Green's function for the flat conducting surface satisfying the boundary equation at $z = 0$

$$\frac{\partial}{\partial z}G_o + \alpha_o G_o = 0. \tag{10}$$

Also note that in (9), $S$ is the area enclosed by the path $C$ as shown in Fig. 2. Equation (9) is then converted into the following random integral equation for $G(r, r_o)$

$$G(r,r_o) = G_o(r,r_o) + \int G_o(r,r_1)V(r_1)G(r_1,r_o)\,dx_1 \tag{11}$$

where $r = r(x,z), r_o = r_o(x_o,z_o)$, and $r_1 = r_1(x_1, z_1 = 0)$. Note that $G_o$ is a deterministic function. However, $V(r_1)$ and $G(r,r_o)$ are random functions.

## V. Dyson's Equation and Coherent Field $\langle G\rangle$

Once we get the integral equation, we can obtain the Dyson's equation for $\langle G\rangle$ [8], [10], [21]. The detailed derivation of Dyson's equation using the diagram method is given in [21] and is not repeated here. Dyson's equation is, therefore

$$\begin{aligned} \langle G(r,r_o)\rangle = G_o(r,r_o) &+ \int G_o(r,r_1) \\ &\times M(r_1,r_2)\langle G(r_2,r_o)\rangle\,dx_1\,dx_2. \end{aligned} \tag{12}$$

This is Dyson's equation which is the fundamental equation for the average field $\langle G\rangle$. The operator $M(r_1,r_2)$ is called the Mass

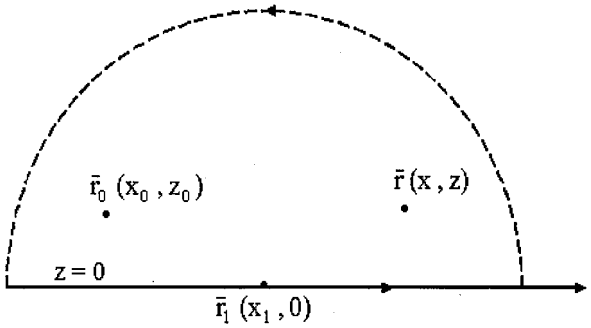


Fig. 2. Random integral equation (11).

operator and in the first-order smoothing approximation is given by [21]

$$M(r_1, r_2) = \langle V(r_1) G_o(r_1, r_2) V(r_2) \rangle = M(r_1 - r_2). \quad (13)$$

Note that $M$ is a function of the difference $r_1 - r_2$ only. We now solve the Dyson's equation (12) using the given Mass operator (13) using the spectral (Fourier transform) method. We express $\langle G \rangle, G_o$ and $M$ in Fourier transforms

$$\langle G(r, r_o) \rangle = \frac{1}{2\pi} \int \langle G(\kappa; z, z_o) \rangle e^{i\kappa(x - x_o)}\, d\kappa \quad (14)$$

$$G_o(r, r_o) = \frac{1}{2\pi} \int G_o(\kappa; z, z_o) e^{i\kappa(x - x_o)}\, d\kappa \quad (15)$$

$$M(r_1 - r_2) = \frac{1}{2\pi} \int M(\kappa; z_1 - z_2) e^{i\kappa(x_1 - x_2)}\, d\kappa. \quad (16)$$

The correlation function of the height $h(x)$ is expressed as

$$\langle h(x_1) h(x_2) \rangle = \int W(\kappa) e^{i\kappa(x_1 - x_2)}\, d\kappa \quad (17)$$

where we assumed $h(x)$ is a homogeneous random function and $W(\kappa)$ is the power spectral density function. In this paper, we use the Gaussian correlation function for $h(x)$ with root-mean-square (rms) height $h_o$ and correlation distance $l$

$$\langle h(x_1) h(x_2) \rangle = h_o^2 e^{-\frac{(x_1 - x_2)^2}{l^2}}$$

$$W(\kappa) = \frac{h_o^2 l}{2\sqrt{\pi}} e^{-\frac{\kappa^2 l^2}{4}}. \quad (18)$$

The Gaussian spectrum is used to verify our analytical results by comparing with numerical Monte Carlo simulations based on the Gaussian spectrum. It should be noted, however, that our results can be used for any spectrum which would be used to represent an actual problem.

## VI. Sommerfeld Pole and Zenneck Wave for a Flat Conducting Surface

First let us express the flat surface Green's function $G_o$ in the well-known Fourier transform [1], [22].

$$G_o(\kappa; z, z_o) = \frac{i}{2k_z} \left( e^{ik_z|z - z_o|} + R_o(\kappa) e^{ik_z(z + z_o)} \right). \quad (19)$$

The reflection coefficient $R_o(\kappa)$ is for the flat conducting surface and is given by

$$R_o(\kappa) = \frac{1 - Q_o}{1 + Q_o} \quad (20)$$

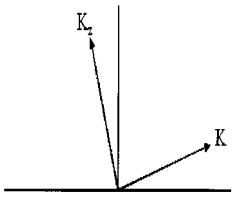


Fig. 3. Somerfeld pole $\kappa$ in the complex plane for flat conducting surfaces.

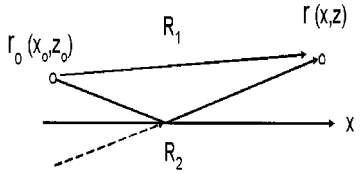


Fig. 4. Geometry for (25) for flat surface.

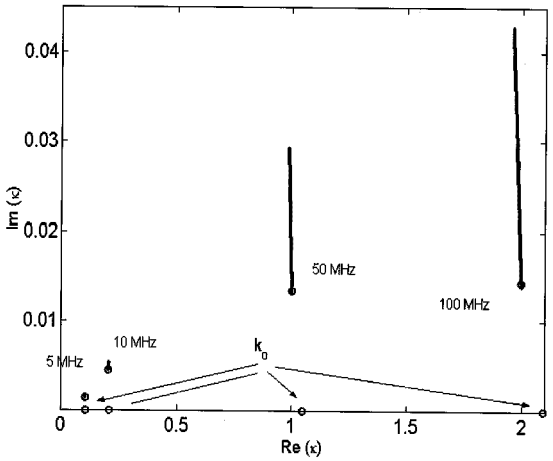


Fig. 5. Case 1: Zenneck wave propagation constant $\kappa$ with $k_o$ for increasing surface roughness $\sigma = 0.0$–$0.3$ m at 5, 10, 50, and 100 MHz.

where $Q_o = (\alpha_o / ik_z) = (k_o / k_z)(Z_s / Z_o)$ and $\kappa^2 + k_z^2 = k_o^2$. The Sommerfeld pole is therefore located at

$$1 + Q_o = 0 \quad (21)$$

or

$$k_z + k_o \left( \frac{Z_s}{Z_o} \right) = 0. \quad (22)$$

Note that the exact Sommerfeld pole is given by

$$k_z + \frac{k_o}{n} \left( 1 - \left( \frac{\kappa}{k_o n} \right)^2 \right)^{1/2} = 0. \quad (23)$$

For grazing angle $\kappa \approx k_o$ and, therefore, we can approximate (23) by (22) with [1]

$$Z_s = \frac{Z_o}{n} \left( 1 - \left( \frac{1}{n} \right)^2 \right)^{1/2}. \quad (24)$$

It is also well known that $k_z$ and $\kappa$ are in the second and first quadrant in the complex plane for the Sommerfeld problem as shown in Fig. 3. The propagation constant for the Zenneck wave

is then given by $\kappa$ satisfying (21). We can now write the complete solution in the following well-known form (Fig. 4):

$$G_o(r, r_o) = G_p(R_1) + G_p(R_2) - 2P \tag{25}$$

where

$$G_p(R) = \frac{i}{4} H_o^{(1)}(k_o R) \approx \frac{1}{4}\left(\frac{2}{\pi k_o R}\right)^{1/2} e^{ikR + i\pi 4} \tag{26}$$

$$P = \frac{1}{2\pi}\int \frac{i}{2k_z}\frac{Q_o(\kappa)}{1+Q_o(\kappa)} e^{ik_z(z+z_o)+i\kappa(x-x_o)}\, d\kappa \tag{27}$$

For large $kR$, we can express (27) in the following well-known form [1], [2]:

$$P = G_p(R_2)[-i\sqrt{\pi p}e^{-p}\operatorname{erfc}(-i\sqrt{p})] \tag{28}$$

where $p$ is the numerical distance given by the difference between the total phase for the Zenneck wave and free-space

$$p = ikR_2 - i[\kappa(x-x_o) + k_z(z+z_o)] \tag{29}$$

with $\kappa$ and $k_z$ evaluated at the Sommerfeld pole. Note that for $e^{jwt}$ time dependence, we should take the complex conjugate of the above formula.

## VII. Coherent Field, Sommerfeld Pole and Zenneck Wave for Conducting Rough Surfaces

We now consider the Sommerfeld problem for the coherent field $\langle G\rangle$ for the rough surface. We express the rough surface Green's function in spectral form and we write

$$\langle G(\kappa; z, z_o)\rangle = \frac{i}{2k_z}\left(e^{ik_z|z-z_o|} + R(\kappa)e^{ik_z(z+z_o)}\right) \tag{30}$$

$$\langle G(r, r_o)\rangle = G_p(R_1) + G_p(R_2) - 2\langle P\rangle \tag{31}$$

where

$$P = \frac{1}{2\pi}\int \frac{i}{2k_z}\frac{Q(\kappa)}{1+Q(\kappa)} e^{ik_z(z+z_o)+i\kappa(x-x_o)}\, d\kappa \tag{32}$$

$$R(\kappa) = \frac{1-Q(\kappa)}{1+Q(\kappa)}. \tag{33}$$

First, we note that the coherent field $\langle G\rangle$ behaves in exactly the same manner as the deterministic flat surface Green's function $G_o$. The difference is that while the surface impedance $Z_s$ is given by (24) for the flat case, the surface impedance for the rough surface is different and needs to be obtained by solving Dyson's equation. Once we solve Dyson's equation, we achieve a new reflection coefficient, a new Sommerfeld pole and finally the new Zenneck wave. The final form of the solution is identical to that for the deterministic case, but with the difference in appearance of the Sommerfeld pole.

Let us now go back to Dyson's equation (12). The substitution of (13)–(16) and (30) into (12) and performing the integration with respect to $x_1$ and $x_2$ we get (Appendix A)

$$1 + R(\kappa) = 1 + R_o(\kappa) + (1 + R_o(\kappa)) \times \int L_1(\kappa', \kappa) W(\kappa - \kappa') L_2(\kappa, \kappa')\, d\kappa' \tag{34}$$

where

$$L_1(\kappa', \kappa) = \frac{M(\kappa', \kappa)}{2}(1 + R_o(\kappa')) + \frac{\alpha_o}{2}(1 - R_o(\kappa')) \tag{35}$$

$$L_2(\kappa, \kappa') = \frac{M(\kappa, \kappa')}{2}(1 + R(\kappa)) + \frac{\alpha_o}{2}(1 - R(\kappa)) \tag{36}$$

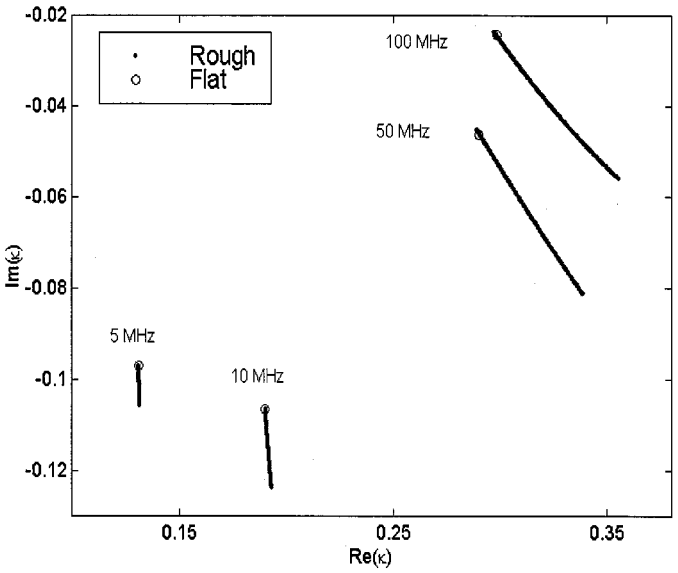


Fig. 6. Case 1: effective surface impedance for Zenneck wave in complex $\kappa$-plane for increasing surface roughness $\sigma = 0.0$–$0.3$ m at 5, 10, 50, and 100 MHz.

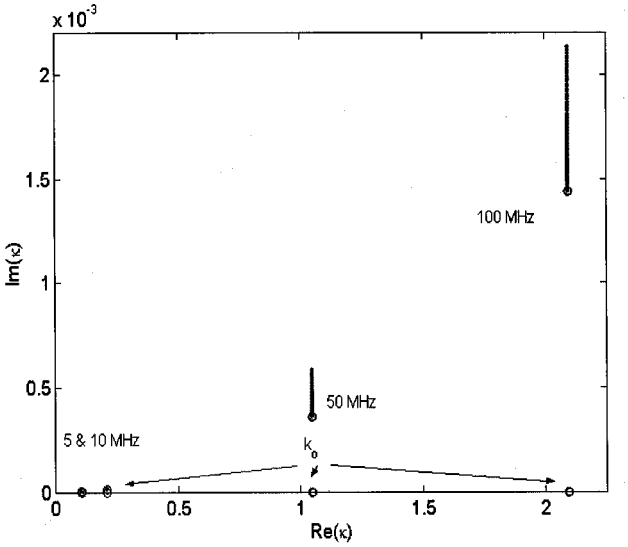


Fig. 7. Case 2: Zenneck wave propagation constant $\kappa$ with $k_o$ for increasing surface roughness $\sigma = 0.0$–$0.2$ m at 5, 10, 50, and 100 MHz.

(37)

and

$$M(\kappa', \kappa) = \frac{i}{k_z'}\left[\kappa\kappa' - k_o^2\right] \tag{38}$$

$$M(\kappa, \kappa') = \frac{i}{k_z}\left[\kappa\kappa' - k_o^2\right]. \tag{39}$$

Rearranging (34), we finally get the reflection coefficient $R(\kappa)$ for the conducting Rough surface

$$R(\kappa) = \frac{1-Q(\kappa)}{1+Q(\kappa)} \tag{40}$$

where

$$Q(\kappa) = \frac{Q_o(\kappa) - \int \mathrm{L}_1(\kappa', \kappa) W(\kappa - \kappa') M(\kappa, \kappa')\, d\kappa'}{1 + \int \mathrm{L}_1(\kappa', \kappa) W(\kappa - \kappa')\alpha_o\, d\kappa'}. \tag{41}$$

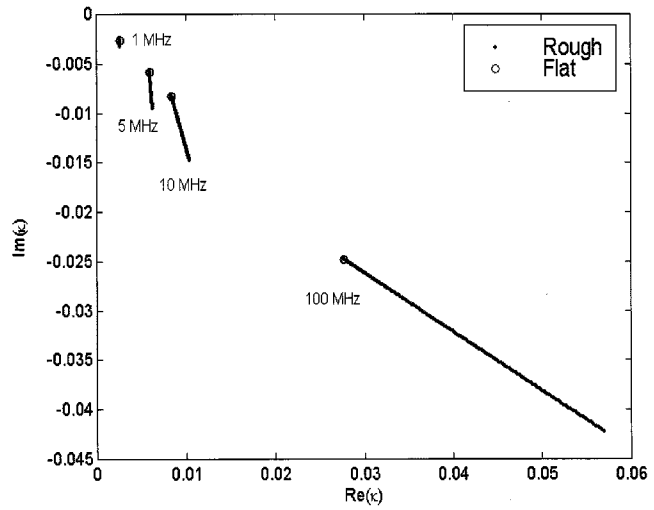


Fig. 8. Case 2: effective surface impedance for Zenneck wave in complex $\kappa$-plane for increasing surface roughness $\sigma = 0.0$–$0.2$ meters at 1, 5, 10, and 100 MHz.

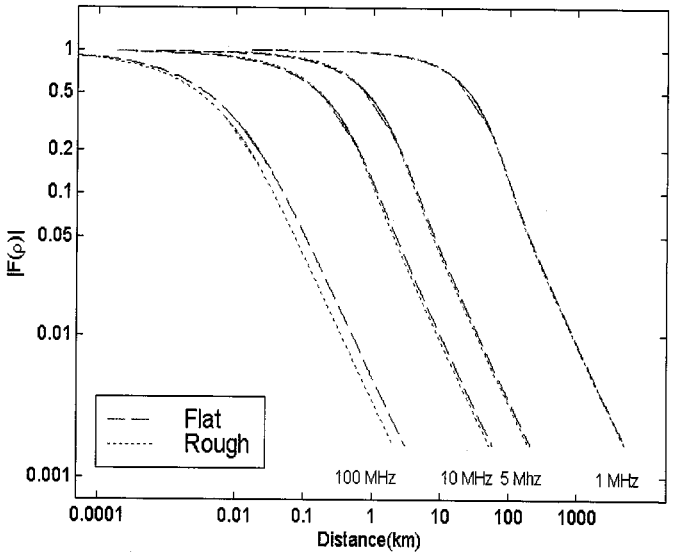


Fig. 9. Case 1: attenuation function $|F(\rho)|$ for flat and rough surface height $\sigma = 0.3$ m at 1, 5, 10, and 100 MHz.

We can now obtain the effective surface impedance $\overline{\Delta(\kappa)}$ for the coherent field

$$\overline{\Delta(\kappa)} = \frac{k_z}{k_o} Q(\kappa). \tag{42}$$

Noting that $\Delta = (k_z/k_o)Q_o(\kappa)$, we write

$$\overline{\Delta(\kappa)} = \frac{\Delta - \frac{k_z}{k_o}\int \mathrm{L}_1(\kappa',\kappa)W(\kappa-\kappa')M(\kappa,\kappa')\,d\kappa'}{1+\int \mathrm{L}_1(\kappa',\kappa)W(\kappa-\kappa')\alpha_o\,d\kappa'} \tag{43}$$

where

$$L_1(\kappa',\kappa) = \frac{M(\kappa',\kappa)+\alpha_o Q_o(\kappa')}{1+Q_o(\kappa')}$$

and $\alpha_o = ik_o\Delta$. In the limit of $\Delta \to 0$, we get

$$\overline{\Delta(\kappa)} = \Delta - \frac{k_z}{k_o}\int M(\kappa',\kappa)W(\kappa-\kappa')M(\kappa,\kappa')\,d\kappa'$$

which agrees with Barrick [4, eq. (24)] when converted to the 1-D surface and evaluated at $\kappa = k_o$.

We now consider the Sommerfeld pole given by

$$1 + Q(\kappa) = 0. \tag{44}$$

With this new Sommerfeld pole, the coherent field $\langle G\rangle$ is given by the same form as that of the flat surface. For large $kR$

$$\begin{aligned}\langle G(r,r_o)\rangle &= G_p(R_1) + G_p(R_2) - 2\langle P\rangle \\ \langle P\rangle &= G_p(R_2)[-i\sqrt{\pi p}e^{-p}\operatorname{erfc}(-i\sqrt{p})]\end{aligned} \tag{45}$$

where $p$ is the numerical distance for the rough conducting surface given by (29) with the new Sommerfeld pole given by (44). In order to find the propagation constant for the Zenneck wave, we first calculate $k_z$. From (41) and (44), we can express $k_z$ as the following:

$$k_z = \frac{-k_o\Delta}{1-\int \mathrm{L}_1(\kappa',\kappa)W(\kappa-\kappa')[M(\kappa,\kappa')-\alpha_o]\,d\kappa'}. \tag{46}$$

For the flat surface case, $k_z = -k_o\Delta$. Therefore, the integral in (46) represents the rough surface effects. Numerical calculations of $k_z$ can be done from (46) using iterations. The propagation constant for the Zenneck wave is then obtained by

$$\kappa = \sqrt{k_o^2 - k_z^2}. \tag{47}$$

We are mainly concerned with the propagation along the surface and the amount of attenuation of the field owing to surface roughness. When both the transmitter and the receiver are on the surface $z = 0$, the rough surface Green's function reduces to

$$\langle G(r,r_o)\rangle = 2G_p(R)F(\rho) \tag{48}$$

where $F(\rho)$ is the attenuation function of the field along the surface and is given by

$$F(\rho) = 1 + i\sqrt{\pi p}e^{-p}\operatorname{erfc}(-i\sqrt{p}). \tag{49}$$

Once the Sommerfeld pole for the rough surface effects has been calculated, the attenuation of the field (49) maybe calculated from the numerical distance (29). In the next section, we calculate the Zenneck pole, the surface impedance, and the attenuation function along the rough surface and compare to a flat surface.

## VIII. Numerical Examples

We now consider two examples of conducting media. Case 1: dielectric constant ($\epsilon = 10, \sigma = 9 * 10^{-3}$), which is representive of land. Case 2: ($\epsilon = 80, \sigma = 4$), which represent a sea media. The media cases are chosen to compare the analytical rough surface results with the flat surface model. The surface spectrum used was Gaussian. Actual propagation over land and sea require more realistic spectra and other consideration as spherical earth models. For this discussion, we restricted the correlation distance to 1.24 m and allowed the rms height to range from $\sigma = 0.0$ to 0.3 m. Thus, the effective range for this theory is between 1–100 MHz. Below these frequencies there is very little surface disturbance and above these frequencies the theory does not apply. We expect the largest deviation to occur at 100 MHz, where the rough surface contributions become appreciable. Other frequency ranges maybe considered by modifying the rough surface height. We are concerned with the effects of rough surface upon the attenuation function $|F(\rho)|$ as a function

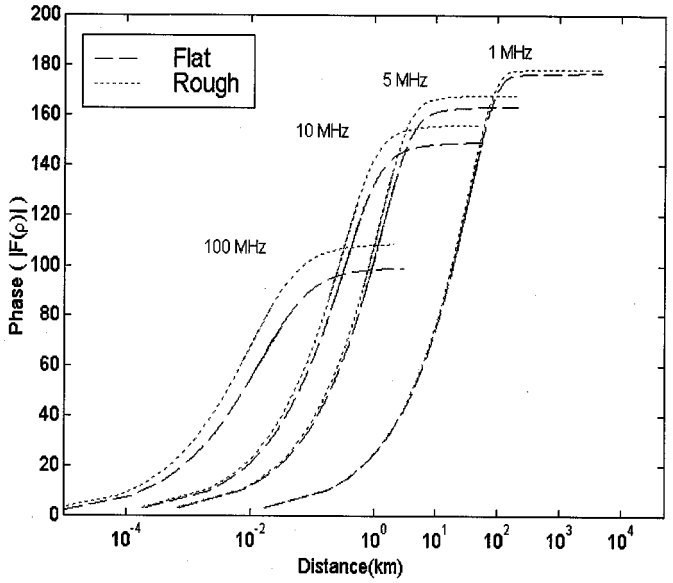


Fig. 10. Case 1: Phase for attenuation function $F(\rho)$ for flat and rough surface height $\sigma = 0.3$ m at 1, 5, 10, and 100 MHz.

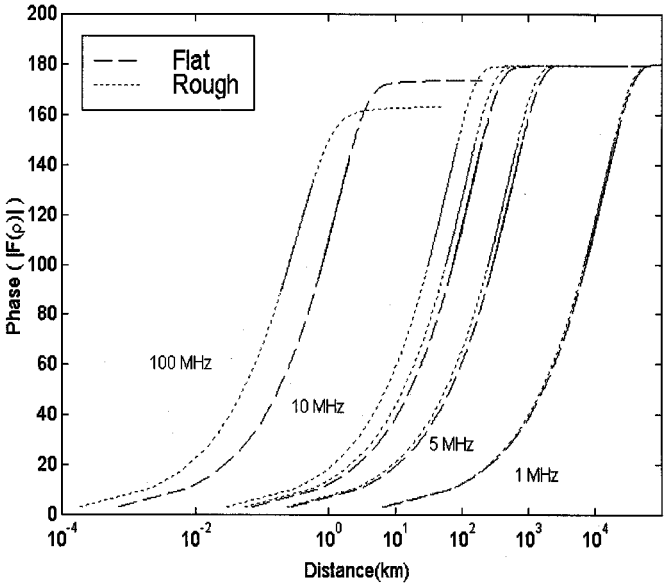


Fig. 12. Case 2: Phase for attenuation function $F(\rho)$ for flat and rough surface height $\sigma = 0.3$ m at 1, 5, 10, and 100 MHz.

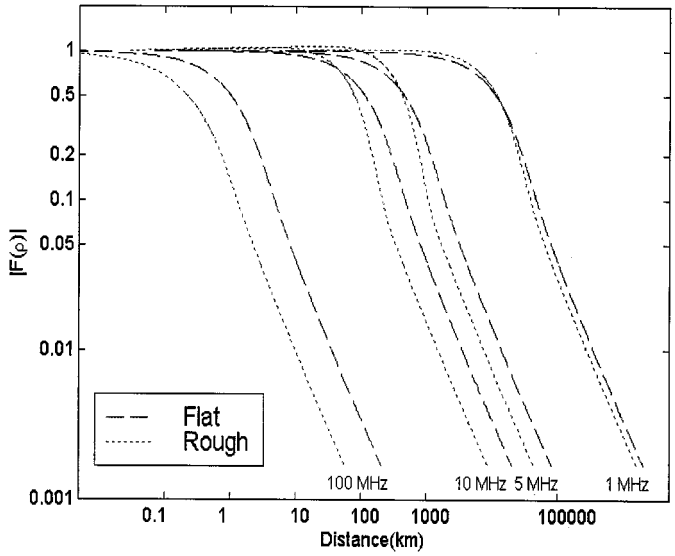


Fig. 11. Case 2: attenuation function $|F(\rho)|$ for flat and rough surface height $\sigma = 0.2$ m at 1, 5, 10, and 100 MHz.

of the real distance. Therefore, we must calculate the Zenneck pole from (46) and (47) to obtain the propagation constant

$$\kappa = \kappa_r + i\kappa_i. \tag{50}$$

This is done through an iterative search from (46). In Fig. 5, the Zenneck wave propagation constants are shown in the complex plane for the frequencies 5, 10, 50, and 100 MHz for land. The figures indicates the deviation of the pole away from the flat surface $(o)$ as the rough surface height $\sigma$ increases from 0.0 to 0.3 m; also included is the free-space wavenumber. Note, that the attenuation (imaginary part) increases with roughness, while the real part remains unaffected. In Fig. 6. we plot the surface impedance for case 1 with increasing roughness from the flat surface. Note that the real part is not changing much, but the imaginary part, which is negative (inductive) increases in magnitude showing more reactive stored energy due to the roughness. In Figs. 7 and 8, the Zenneck wave propagation constant and the surface impedance for case 2 are shown for increasing surface roughness. We now consider the attenuation function (49). In Figs. 9 and 10, the magnitude and phase of the propagation factor (attenuation function) for case 1 as a function of the real distance is given to contrast the effects of surface roughness ($\sigma = 0.3$ m) against the flat surface ($\sigma = 0.0$ m). In Figs. 11 and 12, the propagation factor (attenuation function) for case 2 is shown with the effects of surface roughness ($\sigma = 0.2$ m). As we can see at the lower frequencies, where there is very little surface disturbance, there is almost no difference between the flat and rough surfaces. However, at 100 MHz, the rough surface contributions are significant, and the coherent field attenuates faster than the flat surface case. Finally, a Monte Carlo simulation was conducted using FDTD to simulate the Zenneck wave propagation over the rough surface. In Figs. 13 and 14, a comparison for the normalized attenuation function between the numerical simulation and the theory is given for both case 1 and 2.

## IX. Incoherent Field

Let us now consider the incoherent field. We first note that the total field $G$ consists of the coherent field $\langle G \rangle$ and the incoherent field (or diffuse) $G_d$.

$$G = \langle G \rangle + G_d. \tag{51}$$

In the last section, we considered the coherent field or the first moment of the field. If the surface roughness is small, then the coherent field is dominant. However, as the roughness increases or, at a larger distance from the source, the coherent field diminishes and the incoherent field becomes dominant. In this section, we describe the first-order solution for the incoherent

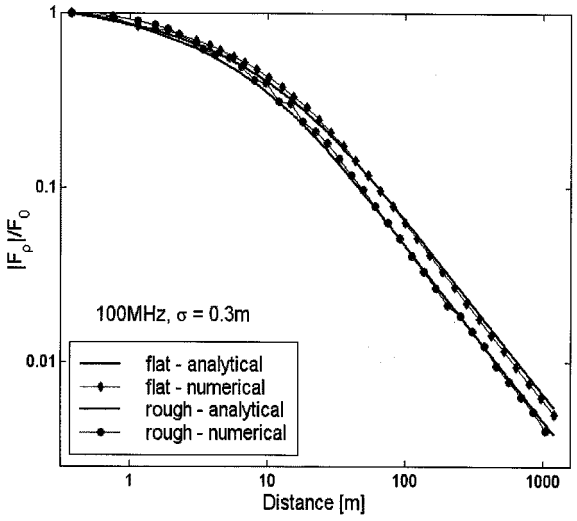


Fig. 13. Comparison between normalized attenuation function for Monte Carlo simulations and theory for Case 1 at 100 Mhz for flat and rough surface height $\sigma = 0.3$ m.

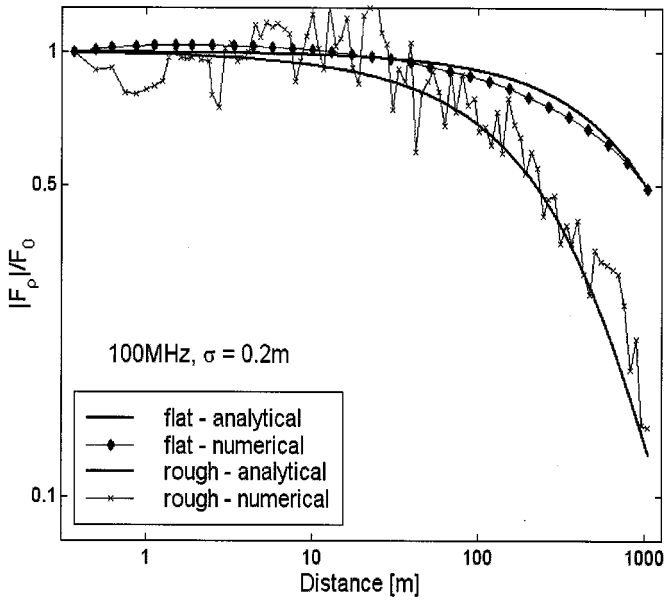


Fig. 14. Comparison between normalized attenuation function for Monte Carlo simulations and theory for Case 2 at 100 MHz for flat and rough surface height $\sigma = 0.2$ m.

field. This requires the evaluation of the second moment or the mutual coherence function. We begin with the fundamental Bethe–Salpeter's equation. This equation describes the correlation of fields at $r$ and $r'$ due to the sources located at $r_o$ and $r'_o$. The correlation of fields is also called the mutual coherence function (MCF), which we describe as (Fig. 15)

$$\Gamma(r,r';r_o,r'_o) = \langle G(r,r_o)G^*(r',r'_o)\rangle. \tag{52}$$

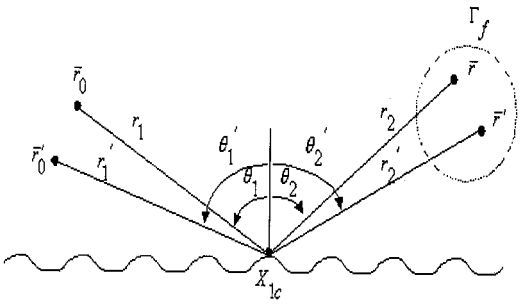


Fig. 15. Incoherent intensity and scattering cross section.

The Bethe–Salpeter's equation describing the propagation of the correlation of fields is then given by

$$\begin{aligned}\langle G(r,r_o)G^*(r',r'_o)\rangle &= \langle G(r,r_o)\rangle\langle G^*(r',r'_o)\rangle \\ &\quad + \int dr_1\, dr'_1 \langle G(r,r_1)\rangle\langle G^*(r',r'_1)\rangle\langle V(r_1)V(r'_1)\rangle \\ &\quad \times \Gamma(r,r';r_o,r'_o)\end{aligned} \tag{53}$$

under the first-order smoothing approximation. The first iteration of this equation is then given by approximation $\Gamma$ in the integrand by the coherent terms. We then rewrite the mutual coherence function into the sum of a coherent $\Gamma_{\rm coh}$ and an incoherent mutual coherence function $\Gamma_f$

$$\Gamma = \Gamma_{\rm coh} + \Gamma_f. \tag{54}$$

The coherent mutual coherence function is given by

$$\Gamma_{\rm coherent} = \langle G(r,r_o)\rangle\langle G^*(r',r'_o)\rangle \tag{55}$$

which was determined from earlier sections. The fluctuating or incoherent mutual coherence function under the first-order smoothing approximation is given by

$$\begin{aligned}\Gamma_f &= \int dr_1\, dr'_1 \langle G(r,r_1)\rangle\langle G^*(r',r'_1)\rangle\langle V(r_1)V(r'_1)\rangle \\ &\quad \times \langle G(r_1,r_o)\rangle\langle G^*(r'_1,r'_o)\rangle\end{aligned} \tag{56}$$

where $V(r_1)$ is given in (8). Substituting the coherent Green's function (30) with (40) and (41), we arrive at the spatial Fourier transform representation of the incoherent mutual coherence function

$$\begin{aligned}\Gamma_f &= \int dx_c \left(\frac{1}{2\pi}\right)^4 \\ &\quad \cdot (2\pi)\int d\kappa\, d\kappa'\, d\kappa_1\, d\kappa'_1 A(\kappa)A^\star(\kappa')W(\kappa_s)B(\kappa_1)B^\star(\kappa'_1) \\ &\quad \times e^{-i(\kappa-\kappa')x_c + i(\kappa_1-\kappa'_1)x_c}\end{aligned} \tag{57}$$

where the elements in the integral are

$$\begin{aligned}A(\kappa) &= \frac{i}{2k_z}(1+R(\kappa))e^{ik_z z + i\kappa x} \\ B(\kappa_1) &= \left[\frac{M}{2}(1+R(\kappa_1)) + \frac{\alpha_o}{2}(1-R(\kappa_1))\right] e^{ik_{z1}z_o - i\kappa_1 x_o} \\ M &= \frac{i}{\kappa_{z1}}\left[\kappa_s\kappa_1 - k_{1z}^2\right] \\ \kappa_s &= \frac{\kappa+\kappa'}{2} - \frac{\kappa_1+\kappa'_1}{2}.\end{aligned} \tag{58}$$

As a special case, we let the source points $r_o = r_o'$, and the observation points $r = r'$; this given the incoherent intensity at $r$ due to the point source at $r_o$. We then get

$$I_f = \langle |G(r, r_o| \rangle = 4k_o \int dx_c |G_p(r, r_c)|^2 \sigma^o(\kappa, \kappa_1) |G_p(r_c, r_o)|^2 \quad (59)$$

where the scattering cross section per unit length of the finitely conducting rough surface is given by (Fig. 15)

$$\sigma^o(\kappa, \kappa_1) = \frac{2\pi}{k_o} \frac{4\, W(\kappa - \kappa_1) |\kappa_s \kappa_1 - \kappa_{1z}^2 - i\kappa_{1z}\alpha_o Q(\kappa_1)|^2}{|1 + Q(\kappa)|^2 |1 + Q(\kappa_1)|^2} \quad (60)$$

where $\kappa_s = \kappa - \kappa_1$.

For Neumann surface, $\alpha_o = 0$ and this is reduced to

$$\sigma^o(\kappa, \kappa_1) = \frac{2\pi}{k_o} \frac{4\, W(\kappa - \kappa_1) |(\kappa\kappa_1 - k_o^2)|^2}{|1 + Q(\kappa)|^2 |1 + Q(\kappa_1)|^2}. \quad (61)$$

This agrees with Fuks *et al.* [19].

## X. Conclusion

In this paper, we discussed the effects of surface roughness on the Sommerfeld propagation problem for a conducting surface. With a rough surface, the field consists of the coherent and the incoherent field. The technique is based on the modified perturbation method and Dyson's equation. The expressions for the new Sommerfeld pole, Zenneck wave, numerical distance, and propagation factors are obtained and numerical examples are conducted, and the analytical results are compared with Monte Carlo simulations. These cases are given to compare the effects of the rough surface to the flat surface case. It is shown that the attenuation of the Zenneck wave increases with roughness and that the surface reactance is inductive and also increasing with roughness. The theory presented here applies to small rough surface heights of less then $0.1\lambda$. Therefore, for a given rms height, the effects of rough surface diminishes at the lower frequencies, while at the higher frequencies, the theory is not applicable. In the intermediate frequencies when the rms height is of the order of $0.1\lambda$, the rough surface effects are significant with increasing attenuation. We then considered the incoherent mutual coherent function and gave a general expression. We also obtained the expression for the scattering cross section per unit length of the rough conducting surface.

## Appendix A

Derivation of (34) from (12). Let us consider the second term of (12)

$$\int G_o(r, r_1) \langle V(r_1) G_o(r_1, r_2) V(r_2) \rangle \langle G(r_1, r_o) \rangle \, dx_1 \, dx_2. \quad (A.1)$$

Expressing in Fourier transform, we write

$$G_o(r, r_o) = \frac{1}{2\pi} \int \frac{i}{2k_z} \left[ e^{ik_z|z - z_o|} + R_o(\kappa) e^{ik_z(z + z_o)} \right] \times e^{i\kappa(x - x_o)} \, d\kappa \quad (A.2)$$

$$G_o(r_1, r_2) = \frac{1}{2\pi} \int \frac{i}{2k_z'} \left[ e^{ik_z'|z_1 - z_2|} + R_o(\kappa') e^{ik_z'(z_1 + z_2)} \right] \times e^{i\kappa'(x_1 - x_2)} \, d\kappa' \quad (A.3)$$

$$\langle h(x_1) h(x_2) \rangle = \int W(\kappa'') e^{-\kappa''(x_1 - x_2)} \, d\kappa'' \quad (A.4)$$

$$\langle G(r_2, r_o) \rangle = \frac{1}{2\pi} \int \frac{i}{2k_z'''} \left[ e^{ik_z'''|z_2 - z_o|} + R(\kappa''') \times e^{ik_z'''(z_2 + z_o)} \right] e^{i\kappa'''(x_2 - x_o)} \, d\kappa'''. \quad (A.5)$$

Now, we examine $V(r_1)$

$$V(r_1) = h_1 \frac{\partial^2}{\partial z_1^2} - \frac{\partial h}{\partial x_1} \frac{\partial}{\partial x_1} + h_1 \alpha_o \frac{\partial}{\partial z_1}. \quad (A.6)$$

Noting (A.6), we recognize the following identities:

$$\frac{\partial^2}{\partial z_1^2} \to (-ik_z')^2 \quad \frac{\partial h_1}{\partial x_1} \to (i\kappa'') h_1$$
$$\frac{\partial}{\partial x_1} \to (i\kappa') \quad \frac{\partial}{\partial z_1} \to (-ik_z').$$

However, we note that while

$$\frac{\partial^2}{\partial z_1^2} \left[ e^{ik_z'(z_2 - z_1)} + R_o(\kappa') e^{ik_z'(z_2 + z_1)} \right] = (-ik_z')^2 \left[ e^{ik_z'(z_2 - z_1)} + R_o(\kappa') e^{ik_z'(z_2 + z_1)} \right]$$

we get

$$\frac{\partial}{\partial z_1} \left[ e^{ik_z'(z_2 - z_1)} + R_o(\kappa') e^{ik_z'(z_2 + z_1)} \right] = (-ik_z') \left[ e^{ik_z'(z_2 - z_1)} - R_o(\kappa') e^{ik_z'(z_2 + z_1)} \right].$$

Thus, for $(\partial/\partial z_1)$, we need to have $-R_o(\kappa')$ instead of $R_o(\kappa')$. Similarly, for $V(r_2)$ we get

$$\frac{\partial^2}{\partial z_2^2} \to (-ik_z''')^2 \quad \frac{\partial h_2}{\partial x_2} \to (-i\kappa'') h_1$$
$$\frac{\partial}{\partial x_2} \to (i\kappa''') \quad \frac{\partial}{\partial z_2} \to (-ik_z''').$$

Also, we need to have $-R_o(\kappa''')$ for the term with $(\partial/\partial z_2)$. Finally, we get for (A.1), expressed in Fourier transforms

$$\int dx_1 \, dx_2 F_1 F_2 F_3 F_4 \quad (A.7)$$

where

$$F_1 = \frac{1}{2\pi} \int G_o(\kappa; z, z_1) e^{i\kappa(x - x_1)} \, d\kappa$$
$$F_2 = \frac{1}{2\pi} \int A(\kappa', \kappa'') e^{i\kappa'(x_1 - x_2)} \, d\kappa'$$
$$F_3 = \int W(\kappa'') e^{i\kappa''(x_1 - x_2)} \, d\kappa''$$
$$F_4 = \frac{1}{2\pi} \int B(\kappa'', \kappa''') e^{i\kappa'''(x_2 - x_o)} \, d\kappa'''$$

and

$$A(\kappa', \kappa'') = \frac{i}{2k_z} \left[ -k_z'^2 + \kappa''\kappa' \right] \left[ e^{ik_z'(z_2 - z_1)} + R_o(\kappa') e^{ik_z'(z_2 + z_1)} \right] + \frac{i}{2k_z'} \left[ -i\alpha_o k_z' \right] \left[ e^{ik_z'(z_2 - z_1)} - R_o(\kappa') e^{ik_z'(z_2 + z_1)} \right] \quad (A.8)$$

$$B(\kappa'',\kappa''') = \frac{i}{2k_z'''}\left[-k_z'''^2-\kappa''\kappa'''\right]\left[e^{ik_z'''(z_o-z_2)}+R(\kappa''')\times e^{ik_z'''(z_o+z_2)}\right] + \frac{i}{2k_z'''}\left[-i\alpha_o k_z'''\right]\left[e^{ik_z'''(z_2-z_1)}-R(\kappa''')e^{ik_z'''(z_o+z_2)}\right]. \tag{A.9}$$

Now we integrate (A.7) with respect to $x_1$ and $\kappa''$ and note that

$$\int dx_1 \to 2\pi\delta(-\kappa+\kappa'+\kappa'')$$
$$\int d\kappa'' \to \kappa'' = \kappa-\kappa'.$$

Similiary, we integrate with respect to $x_2$ and $\kappa'''$ and note

$$\int dx_2 \to 2\pi\delta(-\kappa'-\kappa''+\kappa''')$$
$$\int d\kappa''' \to \kappa''' = \kappa'+\kappa'' = \kappa.$$

We then get

$$\langle G(\kappa)\rangle = G_o(\kappa)+G_o(\kappa)\times\int A(\kappa',\kappa-\kappa')W(\kappa-\kappa')B(\kappa-\kappa',\kappa)\,d\kappa'. \tag{A.10}$$

This can be rewritten as (34).

## ACKNOWLEDGMENT

The authors would like to thank the reviewers for their useful comments.

## REFERENCES

[1] J. R. Wait, "The ancient and modern history of EM ground-wave propagation," *IEEE Antennas Propagat. Mag.*, vol. 40, pp. 7–24, Oct. 1998.
[2] ——, *Waves in Stratified Media*. New York: Pergamon, 1962.
[3] E. Feinberg, "On the propagation of radio waves along an imperfect surface," *J. Phys.*, vol. 8, pp. 317–330, 1944.
[4] D. E. Barrick, "Theory of HF/VHF propagation across the rough sea—Part I: The effective surface impedance for a slightly rough highly conducting surface at grazing incident," *Radio Sci.*, vol. 6, pp. 517–526.
[5] ——, "Theory of HF/VHF propagation across the rough sea—Part II: Application to HF/VHF propagation above the sea," *Radio Sci.*, vol. 6, pp. 527–533.
[6] J. R. Wait, "Appendix C: On the theory of ground wave propagation over a slightly roughned curved earth," in *Electromagnetic Probing in Geophysics*. Boulder, CO: Golem, 1971, pp. 37–381.
[7] A. S. Brykhovetsky and I. M. Fuks, "The effective impedance tensor of a statistically uneven impedance surface," *Izvestya VUZ'ov Radiophysika*, vol. 28, no. 11, pp. 1400–1407, 1985. (in Russian); transl. English, see *Radiophys. Quantum Electron.*, pp. 977–983, 1986.
[8] F. G. Bass and I. M. Fuks, *Wave Scattering for Statistically Rough Surface*. New York: Pergamon, 1979.
[9] A. S. Bryukhovetskii, V. M. Tigrov, and I. M. Fuks, "Effective impedance tensor of statistically rough ideally conducting surface.," *Radiophys. Quantum Electron.*, pp. 703–708, 1985.
[10] V. I. Tatarskii, *Wave Propagation in a Turbulent Medium*. New York: Dover, 1967.
[11] S. M. Rytov, Yu. A. Kravtsov, and V. I. Tatarskii, *Principles of Statistical Radiophysics*. New York: Springer-Verlag, 1987.
[12] J. G. Watson and J. B. Keller, "Refection, scattering and absorption of acoustic waves by rough surfaces," *J. Acoust. Soc. Amer.*, vol. 74, pp. 1887–1894, 1983.
[13] ——, "Rough surface scattering via the smoothing method," *J. Acoust. Soc. Amer.*, vol. 75, pp. 1705–1708, 1984.
[14] S. Ito, "Analysis of scalar wave scattering from slightly rough random surfaces: A multiple scattering theory," *Radio Sci.*, vol. 20, pp. 1–12, 1985.
[15] A. Ishimaru, J. D. Rockway, and Y. Kuga, "Rough surface green's function based on the first order modified perturbation and smoothing diagram method," *Waves Random Media*, vol. 10, no. 1, pp. 17–31, 2000.
[16] "Special issue on low-grazing-angle backscattering from rough surfaces," *IEEE Trans. Antennas Propagat.*, vol. 46, pp. 1–2, Jan. 1998.
[17] D. E. Barrick, "Grazing behavior of scatter and propagation above any rough surface," *IEEE Tran. Antennas Propagat.*, vol. 46, pp. 73–83, Jan. 1998.
[18] ——, "Near-grazing illumination and shadowing of rough surfaces," *Radio Sci.*, vol. 30, pp. 563–580, 1995.
[19] I. M. Fuks, V. I. Tatarskii, and D. E. Barrick, "Behavior of scattering from a rough surface at small grazing angles," *Waves Random Media*, vol. 9, pp. 295–305, 1999.
[20] A. Ishimaru, *Wave Propagation and Scattering in Random Media*. Piscataway, NJ: IEEE, 1997.
[21] U. Frisch, "Wave propagation in random media," in *Probabilistic Methods in Applied Mathematics*, A. T. Bharucha-Reid, Ed. New York: Academic, 1968.
[22] A. Ishimaru, *Electromagnetic Wave Propagation, Radiation and Scattering*. Englewood Cliffs, NJ: Prentice-Hall, 1991.

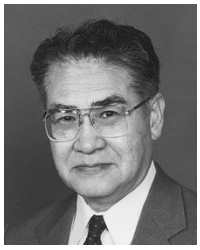

**Akira Ishimaru** (M'58–SM'63–F'73–LF'94) received the B.S. degree in 1951 from the University of Tokyo, Tokyo, Japan, and the Ph.D. degree in electrical engineering in 1958 from the University of Washington, Seattle.

From 1951 to 1952, he was with the Electrotechnical Laboratory, Tanashi, Tokyo, and in 1956, he was with Bell Laboratories, Holmdel, NJ. In 1958, he joined the faculty of the Department of Electrical Engineering of the University of Washington, where he was a Professor of electrical engineering and an Adjunct Professor of applied mathematics. He is currently Professor Emeritus there. He has also been a Visiting Associate Professor at the University of California, Berkeley. His current research includes waves in random media, remote sensing, object detection, and imaging in clutter environment, inverse problems, millimeter wave, optical propagation and scattering in the atmosphere and the terrain, rough surface scattering, and optical diffusion in tissues. He is the author of *Wave Propagation and Scattering in Random Media* (New York: Academic, 1978; IEEE-Oxford University Press Classic reissue, 1997) and *Electromagnetic Wave Propagation, Radiation, and Scattering* (Englewood Cliffs, NJ: Prentice-Hall, 1991). He was Editor (1979–1983) of *Radio Science* and Founding Editor of *Waves in Random Media*, Institute of Physics, U.K.

Dr. Ishimaru has served as a member-at-large of the U.S. National Committee (USNC) and was chairman (1985–87) of Commission B of the USNC/International Union of Radio Science. He is a Fellow of the Optical Society of America, the Acoustical Society of America, and the Institute of Physics, U.K. He was the recipient of the 1968 IEEE Region VI Achivement Award and the IEEE Centennial Medal in 1984. He was appointed as Boeing Martin Professor in the College of Engineering in 1993. In 1995, he was awarded the Distinguished Achievement Award from the IEEE Antennas and Propagataion Society. He was elected to the National Academy of Engineering in 1996. In 1998, he was awarded the Distinguished Achievement Award from the IEEE Geoscience and Remote Sensing Society. He is the recpient of the 1999 IEEE Heinrich Hertz Medal and the 1999 URSI Dellinger Gold Medal. In 2000, he received the IEEE Third Millennium Medal.

**John Dexter Rockway** received the B.S. degree in physics from the University of California, San Diego, in 1995. He is currently working toward the Ph.D. degree in electrical engineering from the University of Washington, Seattle.

His research interests include rough surface and random media scattering and implementation of theory in computer models for application to imaging and antenna performance.

**Yasuo Kuga** (S'79–M'83–SM'90) received the B.S., M.S., and Ph.D. degrees from the University of Washington, Seattle, in 1977, 1979, and 1983, respectively.

He is currently a Professor of electrical engineering at the University of Washington. From 1983 to 1988, he was a Research Assistant Professor of electrical engineering at the University of Washington. From 1988 to 1991, he was an Assistant Professor of electrical engineering and computer science at the University of Michigan, Ann Arbor. Since 1991, he has been with the University of Washington. He was an Associate Editor of *Radio Science* (1993–1996). His research interests are in the areas of microwave and millimeter-wave remote sensing, high-frequency devices, and optics.

Dr. Kuga is an Associate Editor of the IEEE TRANSACTIONS ON GEOSCIENCE AND REMOTE SENSING (1996–2000). He was selected the 1989 Presidential Young Investigator.

**Seung-Woo Lee** received the B.S. and M.S. degrees in electrical engineering from Seoul National University, Korea, in 1994 and 1996, respectively. He is currently working toward the Ph.D. degree in electrical engineering from the University of Washington, Seattle.